

## A bilayer of Wigner crystal in the harmonic approximation

This article has been downloaded from IOPscience. Please scroll down to see the full text article.

1995 J. Phys.: Condens. Matter 7 7217

(<http://iopscience.iop.org/0953-8984/7/36/011>)

View [the table of contents for this issue](#), or go to the [journal homepage](#) for more

Download details:

IP Address: 171.66.16.151

The article was downloaded on 12/05/2010 at 22:05

Please note that [terms and conditions apply](#).

# A bilayer of Wigner crystal in the harmonic approximation

Keivan Esfarjani and Yoshiyuki Kawazoe

Institute for Materials Research, Tohoku University, Sendai 980-77, Japan

Received 12 May 1995, in final form 19 June 1995

**Abstract.** Using the harmonic approximation as a model to describe a bilayer of a Wigner crystal in wide quantum wells, we calculate the ground state properties and the phonon spectrum of this system as a function of the density and layer separation. A fitting formula is given for the ground state energy.

## 1. Introduction

Many properties of a bilayer of an electron liquid in a magnetic field and a wide quantum well have been discussed over the past few years [1]. However, the properties of the solid phase remain to be investigated. Several properties of *one layer* of a Wigner solid (with and without a magnetic field) such as the phonon spectrum and zero-point energy in the harmonic approximation [2, 3], anharmonic corrections to the phonons [4, 5] and shear modulus [6, 7] have already been calculated in the past by Esfarjani among others. Mean-field methods such as the time-dependent Hartree–Fock theory [8] and quantum Monte Carlo simulations [9, 10] have also been used to describe this system. Therefore there is a rather good understanding of the properties of the solid phase, and the validity and limits of different theories. In a first attempt, we use the simplest model to describe this system. The well is represented by a quadratic potential along the  $z$  direction and the Hamiltonian is replaced by a harmonic one, so that it can be exactly diagonalized. Higher anharmonic corrections, as well as the exchange are neglected; however, this theory includes electron correlations and the motion of electrons perpendicular to the layers (the wavefunction has a finite  $z$  extent), and is therefore three dimensional, and better than the mean-field type of approach.

The bilayer system is present in wide quantum wells or heterostructures in which there could be a barrier separating two wells. It must be emphasized that the background positive charge coming from the donor impurities and the metallic gates parallel to the two-dimensional plane must be present on both sides of the well, otherwise it is electrostatically impossible to have two separate electron layers with a positive plate of opposite charge on only one side of them. In this case, the two layers are formed because of the Coulomb repulsion between the electrons, each layer screening its neighbouring positive plate. In what follows, we assume two plates of the same charge, so that the two electron layers have the same density. We have omitted from our energy terms a constant term coming from the gate interaction equal to  $2\pi b/ac$ ,  $b$  being the distance between the two gates, and  $ac$  the electron density (this is the well known electrostatic energy of a capacitor).

In this paper, we describe our simple harmonic model representing the solid phase of the bilayer in the quantum well, and present the results of our calculations of the phonon spectrum and total energy of this system.

## 2. Harmonic model

The well perpendicular to the plane is modelled by a parabolic potential  $V(z) = Kz^2/2$ . We furthermore expand the potential energy in powers of the displacements around the equilibrium lattice positions, and keep only up to second-order terms. This is called the harmonic approximation. The resulting Hamiltonian can be reduced to a harmonic oscillator Hamiltonian which can be exactly diagonalized. The resulting eigenvalues are then the phonon energies representing the excitations of the ground state, and one half of their sum is the zero-point energy correction to the classical Coulomb term.

So if we denote the equilibrium lattice positions by  $R_i$ , and the displacements about them by the three-dimensional vector  $\xi_i$ , the Hamiltonian in atomic units ( $\hbar = e = m = 1$ ) becomes

$$H = \sum_{i\sigma} \left[ \frac{P_{i\sigma}^2}{2} + \frac{1}{2} K ((-1)^\sigma d/2 + \xi_{i\sigma}^z)^2 \right] + \frac{1}{2} \sum'_{ij,\sigma\sigma'} \frac{1}{|R_i + \xi_{i\sigma} - R_j - \xi_{j\sigma'} + \Delta_{\sigma\sigma'}|} \quad (1)$$

where the index  $\sigma$  labels the layer, and takes the two values  $+1$  or  $-1$ , and  $\Delta_{\sigma\sigma'}$  is zero if  $\sigma = \sigma'$  and equal to  $d\hat{z} + \Delta$  otherwise.  $d$  is the interlayer distance, and  $\Delta$  is the relative shift of one layer with respect to the other. In the above and what follows, the ' on the sum indicates that the terms  $i = j$  and  $\sigma = \sigma'$  must be excluded from the sum.

The above Hamiltonian contains two terms, the classical energy (obtained for  $\xi_i = 0$  and  $P_i = 0$ ) and the harmonic Hamiltonian  $H_{\text{har}}$ :

$$H_{\text{har}} = \sum_{i\sigma} \left[ \frac{P_{i\sigma}^2}{2} + \frac{1}{2} K ((-1)^\sigma d \xi_{i\sigma}^z + (\xi_{i\sigma}^z)^2) \right] + \frac{1}{2} \sum'_{ij,\sigma\sigma'} \frac{1}{2!} \xi_{i\sigma} \xi_{j\sigma'} : \nabla \nabla \frac{1}{|R_i - R_j + \Delta_{\sigma\sigma'}|}. \quad (2)$$

Hence, we have a two-dimensional lattice with two electrons per unit cell, each in one layer and having three degrees of freedom. This will lead, as we will see, to a  $6 \times 6$  dynamical matrix.

The lattice being invariant under finite translations, we go to the normal modes to separate the Hamiltonian into independent parts. The normal modes are defined by

$$\xi_k = \frac{1}{\sqrt{N}} \sum_i \xi_i e^{ikR_i}$$

$$P_k = \frac{1}{\sqrt{N}} \sum_i P_i e^{-ikR_i}$$

where  $N$  is the number of particles in *one* layer. After substitution in equation (2), we get  $H_{\text{har}} = \sum_k H_k$ , where

$$H_k = \sum_{\sigma} \frac{P_{k\sigma}^2}{2} + \frac{1}{2} \sum_{\sigma\sigma'} \xi_{k\sigma}^\alpha \xi_{-k\sigma'}^\beta D_{\sigma\sigma'}^{\alpha\beta}(k). \quad (3)$$

In the above,  $D$  is the dynamical matrix given by

$$D_{\sigma\sigma'}^{\alpha\beta}(k) = \delta_{\sigma\sigma'} \left[ \sum_i \nabla \nabla \frac{1}{|R_i + \Delta + d\hat{z}|} + \sum_i' (1 - e^{-ikR_i}) \nabla \nabla \frac{1}{|R_i|} + K \delta_{\alpha z} \delta_{\beta z} \right]$$

$$- (1 - \delta_{\sigma\sigma'}) \left[ \sum_i e^{-ikR_i} \nabla \nabla \frac{1}{|R_i + \Delta + d\hat{z}|} \right]. \quad (4)$$

For the sake of brevity, the subscripts  $\alpha$  and  $\beta$  were dropped from the  $\nabla$  signs. Notice that the  $x$  and  $y$  components in the diagonal part of  $D$  contain the dynamical matrix of the 2D Wigner crystal [2] confined to move in the plane (second term of the first bracket).

As can be seen from equation (4), the calculation of the dynamical matrix involves two-dimensional sums of the type  $w(k, \Delta, d) = \sum_i e^{ikR_i} \nabla \nabla |R_i + \Delta + d\hat{z}|^{-1}$ ; likewise, the calculation of the classical energy involves  $e(\Delta, d) = \sum_i |R_i + \Delta + d\hat{z}|^{-1}$ . To make them rapidly convergent, the above terms were calculated by the means of the Ewald sum technique which involves two sums: one sum is the short-range part of the expression and is done in real space, and the other includes the long-range and smooth part of the expression, and is done in reciprocal space.

The eigenvalues of  $D$  are the squares of the phonon frequencies. For large  $K$ , one can identify the highest two modes as being electrons vibrating perpendicular to the plane.

To calculate the dynamical matrix, one must first determine the interlayer distance  $d$ , and the basis vectors  $R_i$ , which characterize the lattice type, as well as  $\Delta$ , the displacement of one layer with respect to the other. This is done by minimizing the total classical energy with respect to  $d$ ,  $R_i$  and  $\Delta$ . The classical energy per particle comes from equation (1) in which  $P_i = 0$  and  $\xi_i = 0$ ,

$$\begin{aligned} \frac{E_{\text{class}}}{2N} &= \frac{1}{2} \sum_i \frac{1}{|R_i + \Delta + d\hat{z}|} + \frac{1}{2} \sum_i' \frac{1}{|R_i|} - \text{positive background term} + \frac{1}{2} K \left( \frac{d}{2} \right)^2 \\ &= \frac{1}{2} E_{\text{other layer}} + \frac{1}{2} E_{\text{Madelung}} + E_{\text{well}}. \end{aligned} \quad (5)$$

This minimization is done numerically with a standard minimization routine [11]. To find the absolute minimum, we started from four different initial configurations in which the system has no symmetry, but is close to respectively a square, rectangle, triangle and rhombohedron with obtuse angle. The shift  $\Delta$  was also taken randomly. We found that the distance  $d$  is generally the same, regardless of the found minimum, and that it scales as  $\sqrt{ac} f(Z_0)$ , where  $ac$  is the area of the unit cell,  $Z_0 = K^{(-1/3)} ac^{(-1/2)}$  is a dimensionless parameter characterizing the well width along the  $\hat{z}$  direction and  $f$  a universal function independent of  $ac$ . This function is displayed in figure 1, and can be approximated by a straight line for wide enough wells ( $Z_0 > 0.32$ ), although its asymptotic form is  $4\pi Z_0^3$ . It was also found that the shift of one layer with respect to the other, characterized by  $\Delta$ , is such that one lattice sits at the centre of the other. Due to the flatness of the interlayer potential for large distances  $d$ , the convergence to the exact centre was accurate to within a few per cent, however.

We also show in figure 2 the plot of the classical energy times  $\sqrt{ac}$  as a function of  $x = d/\sqrt{ac}$ . One can notice that it is a smooth and continuous function even at the monolayer-bilayer transition, even though  $d$  is discontinuous. One can continue this analysis further by computing the classical energy of the trilayer. There would be more degrees of freedom: the structure of the middle layer as well as its density could be different from the outer layers. One can thus find the region over which the bilayer is stable with respect to the interlayer Coulomb interaction. Clearly, for narrow wells the binding energy of one layer is larger than the effect of interlayer repulsion, and for very wide wells ( $d \gg \sqrt{ac}$ ) one expects to get more than two layers. We have done the calculation of the energy of three layers of the same density, and we found that its energy becomes lower than the bilayer for  $x \geq 1.2$ .

In this analysis, the Bohr radius  $a_B (= \epsilon/m^*$  in atomic units) is irrelevant, and all the results are functions of only one dimensionless parameter  $Z_0$  or equivalently  $x = d/\sqrt{ac}$ .  $a_B$ , measuring the length scale where the kinetic energy would be equal to the potential

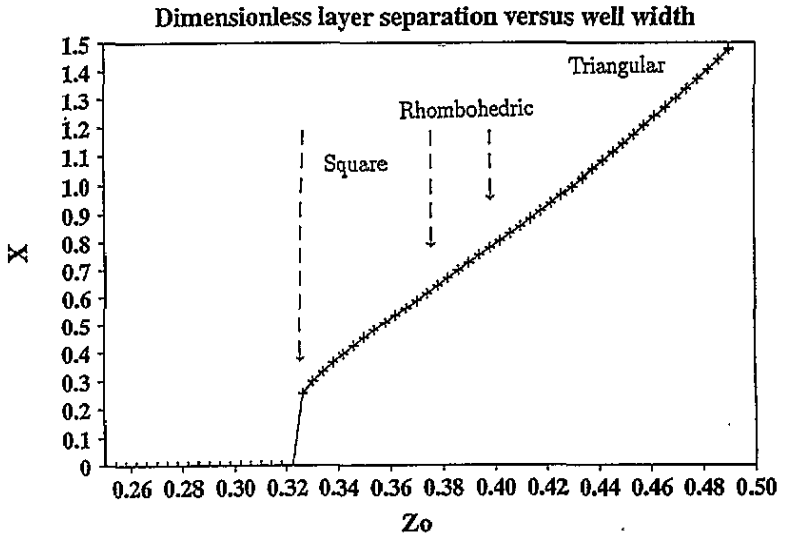


Figure 1. Layer separation  $x = d/\sqrt{ac}$  versus well width characterized by  $Z_0$ .

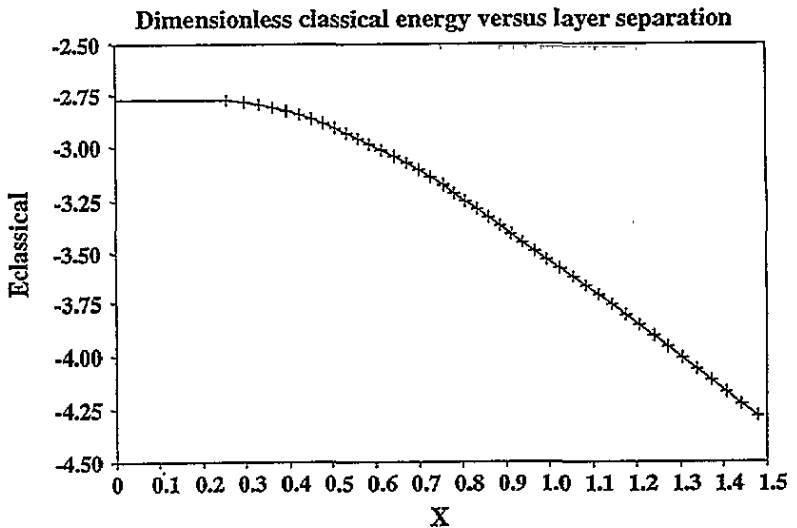


Figure 2. Classical energy times  $\sqrt{ac}$  versus layer separation  $x$ . The fits are not shown on this figure.

energy, becomes important when one includes the kinetic energy. Therefore for the discussion of the total energy (classical + zero point) the system would be characterized by two dimensionless parameters formed from the combination of  $d$ ,  $\sqrt{ac}$  and  $a_B$ .

Confining ourselves to the calculation of the classical energy of the solid bilayer (i.e. with a periodic structure of two electrons per unit cell), we find that for narrow wells ( $Z_0 < 0.32$ ) the monolayer with the triangular structure has lowest energy; this can also be viewed as a centred rectangular structure with aspect ratio  $\sqrt{3}$ . As  $Z_0$  is increased, (i.e. the well gets wider) the interlayer distance  $d$  jumps suddenly to a non-zero value of  $0.27\sqrt{ac}$  and the structure becomes a centred square until  $Z_0$  reaches 0.37 (corresponding

to  $d = 0.61\sqrt{ac}$ . Then the 90 degrees angle of the square decreases continuously to 60 at  $Z_0 = 0.39$  where  $d = 0.75\sqrt{ac}$ . This represents two triangular structures in each layer, and is the limit of weakly interacting layers. For wider wells, this structure remains unchanged until a transition to three layers occurs.

The classical energy per particle can be shown from equation (5) to have the following general form:

$$\frac{E_{\text{class}}}{2N} = \frac{1}{2}e_{\text{Madelung}}/\sqrt{ac} - \pi d/ac + \frac{1}{2}K(d/2)^2 + e_{\text{rest}}$$

where  $-2\pi d/ac$  is the interaction with the other layer in the large- $d$  limit (this can be trivially deduced from Gauss's law). We will therefore use the following fitting formula for the classical energy of the bilayer. The classical energy per particle can be fitted with the one of the two following formulas:

$$\frac{E_{\text{class}}}{2N} = \frac{1}{\sqrt{ac}}(c_0 + c_1x + c_2e^{-\lambda x^2}) \quad (6)$$

or

$$\frac{E_{\text{class}}}{2N} = \frac{1}{\sqrt{ac}}(a_0 + a_1x + a_2x^2 + a_3x^3). \quad (7)$$

In the above  $x = d/\sqrt{ac}$ , and the numerical values of the fitting parameters can be found in table 1. For a triangular structure,  $e_0$  would be  $-3.921/2$ , half of the Madelung energy of this type of lattice, but since the square lattice is also stable for lower  $x$ , we use fitting constants  $e_0$  and  $e_1$ . Although both fits yield similar errors, we prefer the first form because it has the right 'asymptotic' behaviour and is more valid outside the range  $x \geq 1.2$ .

Table 1. Fitting coefficients of the classical and the zero-point energies

| Classical energy |          | Zero-point energy |          |       |           |
|------------------|----------|-------------------|----------|-------|-----------|
| $a_0$            | -2.83785 | $c_0$             | -1.9749  | $b_0$ | 5.73024   |
| $a_1$            | 0.719671 | $c_1$             | -1.5606  | $b_1$ | -3.45517  |
| $a_2$            | -1.98508 | $c_2$             | -0.55193 | $b_2$ | 1.69187   |
| $a_3$            | 0.568521 | $\lambda$         | 5.2838   | $b_3$ | -0.290987 |

### 3. Zero-point energy and mean lattice vibrations

Once the minimum-energy configuration is found with respect to the layer separation and shift as well as lattice structure, we proceed to diagonalize the dynamical matrix which is now assured to be positive definite. In contrast to the classical energy, the zero-point energy (ZPE) is not a continuous function of  $Z_0$ . However, it is found that regardless of the density, the ZPE is a universal function of  $Z_0$  divided by  $(ac)^{3/4}$ . For  $d = 0$  this is a well known property of the 2D Wigner solid. We find here that, for the bilayer case as well, this scaling holds since  $x = d/\sqrt{ac}$  is also a unique function of  $Z_0$ . In this regime, where the structure goes from square at lower  $Z_0$  to triangular at higher  $Z_0$ , the ZPE per particle can be simply fitted with the following formula (see figure 3 and table.1 for  $b_i$ ):

$$\frac{\text{ZPE}}{2N} = \frac{1}{2N} \sum_{k,\lambda} \frac{\omega_{k\lambda}}{2} = \frac{1}{(ac)^{3/4}}(b_0 + b_1x + b_2x^2 + b_3x^3) \quad (8)$$

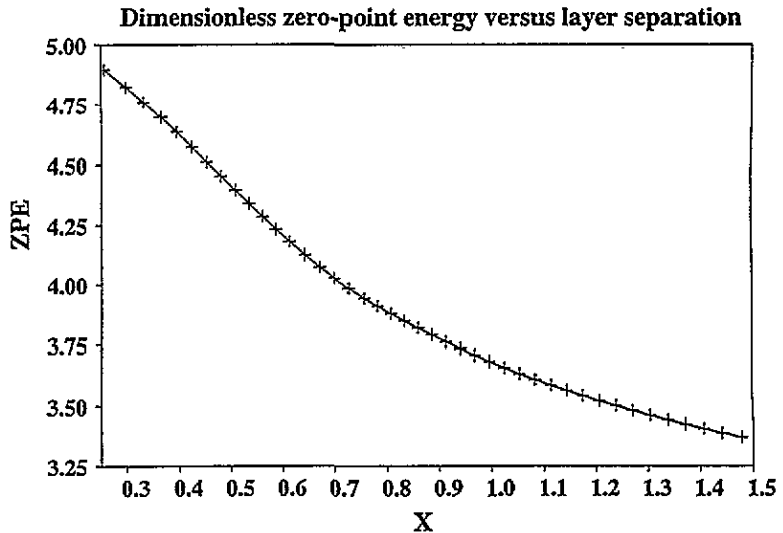


Figure 3. Zero-point energy times  $(ac)^{3/4}$  versus layer separation  $x$ . The fit is not shown on this figure.

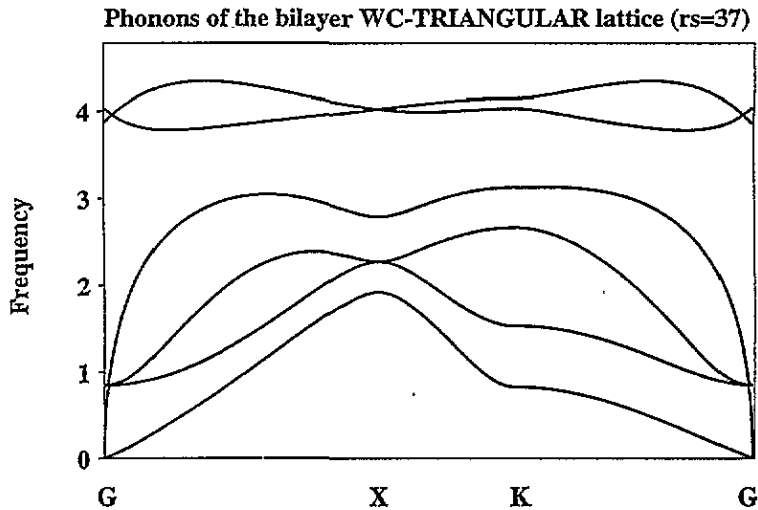


Figure 4. Typical phonon dispersion relation for the triangular lattice at  $Z_0 = 0.407$  and  $x = 0.84$ . The frequency is in units of  $(ac)^{-3/4}$ .

where  $\lambda = 1, 6$  corresponds to the eigenmodes of the dynamical matrix.

Two typical phonon dispersion relations for the square and the triangular lattice are displayed in figures 4 and 5 at  $r_s = \sqrt{ac/\pi}/a_B = 37$  (this corresponds to the melting density of the monolayer Wigner lattice [9]). For small enough well widths, one can identify the two higher branches as the modes of vibration perpendicular to the planes, i.e. along the  $z$  direction. The four lower branches are splittings of the monolayer transverse and longitudinal bands, the lowest one being a shear mode, and the highest one (fourth band) a plasmon-like mode (proportional to  $\sqrt{k}$  at small  $k$ ). In both of these modes where  $\omega(k) \rightarrow 0$  for  $k \rightarrow 0$ , the electrons of each layer vibrate in phase. The two remaining branches (the

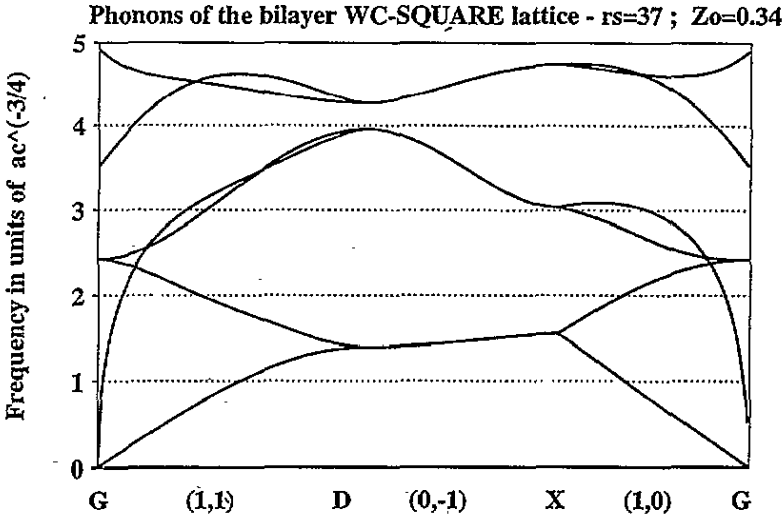


Figure 5. Typical phonon dispersion relation for the square lattice at  $Z_0 = 0.346$  and  $r_s = 37$ . The frequency is in units of  $(ac)^{-3/4}$ .

second and third) have a gap at the  $\Gamma$  point; they correspond to ‘optical’ modes i.e. the two electrons of each layer vibrate in the  $x-y$  plane in opposite directions; the value of the gap representing the strength of interlayer correlations scales like the phonon frequencies, as  $(ac)^{-3/4}$ , and is almost an exponentially decreasing function of  $x$  or  $d$ . Figure 6 shows the variation of the non-zero modes with respect to  $Z_0$ . Two of these modes correspond to motions in the  $z$  direction, and the two others, which are doubly degenerate in the square and triangular structures, represent the ‘optical’ modes. In the monolayer case ( $Z_0 < 0.32$ ), these two modes are of course independent of  $Z_0$ , and one can see that one of the modes along  $z$  goes to zero at the transition point. One can notice the discontinuities corresponding to structural phase transitions, which are specific to the solid phase!

To get an idea about the stability of the lattice, we calculated the mean lattice vibrations (MLV) as well. This quantity is defined as  $MLV = \sqrt{\langle \xi^2 \rangle} / ac$ , where

$$\langle \xi^2 \rangle = \frac{1}{2Nn_0} \sum_{k,\lambda} \frac{1}{\omega_{k\lambda}} \tag{9}$$

and  $n_0$  is the number of layers or more generally the number of species per unit cell.

If we take  $MLV = 0.3$  as a criterion for the stability of the solid phase [13], we can deduce a phase boundary separating the solid from the liquid phase. Figure 7 shows the phase boundary obtained in the  $d/\sqrt{ac}-r_s$  plane ( $ac = \pi r_s^2 a_B^2$ ). This boundary is however obtained for the model adopted above, namely a bilayer in a parabolic well. But it can certainly indicate qualitatively in what region the melting transition takes place. Note that for large values of  $d/\sqrt{ac}$  this ceases to be valid because the bilayer becomes unstable towards the formation of three layers.

We can also study different components of MLV as a function of  $Z_0$  and  $ac$ . For example the displacements in the  $Z$  direction are given by  $\langle \xi_{\perp}^2 \rangle = (1/2Nn_0) \sum_{k,\lambda=5,6} 1/\omega_{k\lambda}$  or the displacements in the  $X-Y$  plane are  $\langle \xi_{\parallel}^2 \rangle = (1/2Nn_0) \sum_{k,\lambda=1,4} 1/\omega_{k\lambda}$ . We show in figure 8 the three quantities  $\sqrt{\xi_{\perp}^2/d^2}$ ,  $\sqrt{\xi_{\parallel}^2/ac}$  and  $\sqrt{\xi^2/(ac+d^2)}$  versus  $x = d/\sqrt{ac}$  for  $r_s$  (one layer) = 37. Because the phonon frequencies scale as  $(ac)^{-3/4}$ , one can also



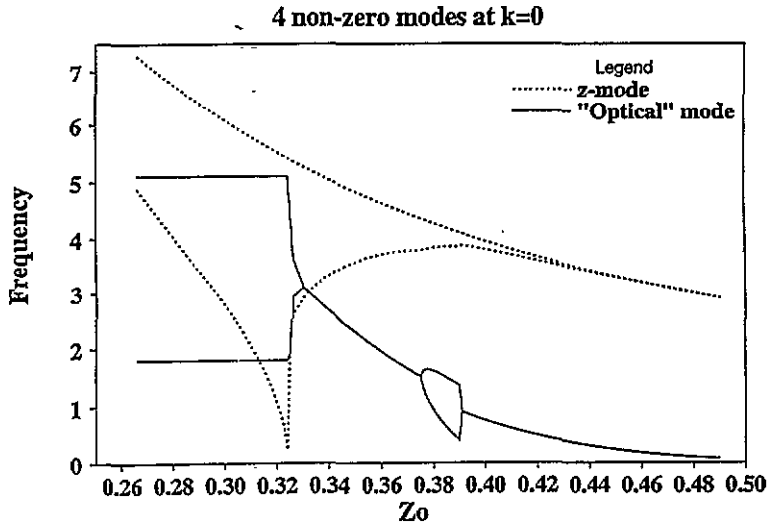


Figure 6. Frequency of the non-zero modes times  $(ac)^{3/4}$  at the  $\Gamma$  point, as a function of  $Z_0$  at  $r_s = 37$ . For a fixed  $Z_0$ , these values scale as  $(ac)^{-3/4}$ . Solid lines are in-plane modes, doubly degenerate for the square and the triangular lattice. The highest mode in the dotted line is the one in which the two electrons move together (in phase) perpendicular to the plane. The other dotted line represents the out-of-plane vibrations whose phases differ by  $\pi$ .

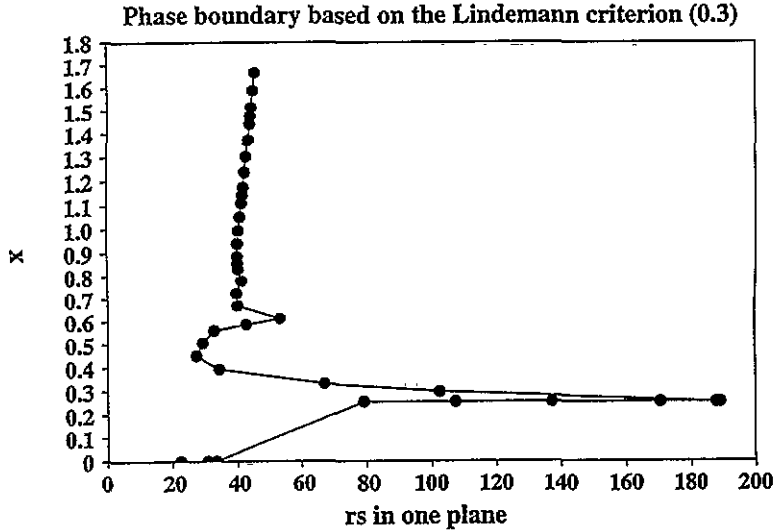


Figure 7. Monolayer-bilayer phase boundary in the  $r_s$ - $x$  plane obtained from the Lindemann criterion (largest component of MLV less than 0.3). Note that for large  $x$  ( $\geq 1.2$ ) there is another instability towards the formation of three layers which is not included in this figure.

deduce a scaling relation for the mean lattice vibrations:  $MLV \propto (ac)^{-1/4}$  (for constant  $Z_0$  or  $x$ ). Notice that the in-plane vibration curve has two humps at  $x = 0.6$  and  $0.74$ . These correspond to the transitions from respectively square lattice to rhombohedral (aspect ratio unity but angle varying continuously from 90 to 60 degrees) and from rhombohedral to triangular structures. We find that it is an intrinsic property of the solid phase in the harmonic

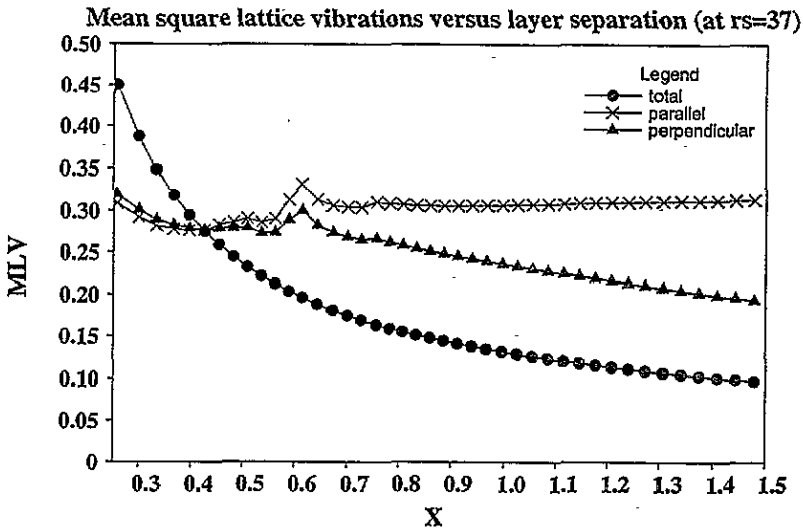


Figure 8. The three mean square lattice vibrations  $\sqrt{\langle \xi_{\perp}^2 \rangle / d^2}$ ,  $\sqrt{\langle \xi_{\parallel}^2 \rangle / ac}$  and  $\sqrt{\langle \xi^2 \rangle / (ac + d^2)}$  versus layer separation  $x$  at  $r_s = 37$ .

approximation that there is some kind of instability at these layer spacings, corresponding to a hump in the MLV, and a discontinuity in the phonon gap at the  $\Gamma$  point. This also occurs at the monolayer–bilayer transition where  $x = 0.25$ . In this region, we suspect, given the large values of  $\langle \xi_{\parallel}^2 \rangle$  and  $\langle \xi_{\perp}^2 \rangle$  that either the harmonic theory breaks down, or, more generally, that the solid phase is unstable (unless one goes to much lower densities; see figure 7).

#### 4. Conclusions

We have developed a harmonic theory for a bilayer of a Wigner crystal. Even though the harmonic theory does not tell us much about the transition to a liquid (it is indeed stable far into the liquid phase, the MLV becoming unreasonably large however), it is a good description of the solid for the three following reasons.

(i) Anharmonic corrections to the harmonic frequencies and total energy were found to be small in the case of the *monolayer* [4, 7]. The next-order corrections in a perturbation expansion of the total energy turn out to consist of two terms of opposite signs which partially cancel each other out. The cubic correction was found to be larger in magnitude than the quartic term. This led to lower phonon frequencies (typically by 10%) and a decrease in the total energy (typically equal to 5% or less of the ZPE) in good agreement with the Green function Monte Carlo results of Tanatar and Ceperley [9]. Therefore we expect that in the bilayer case, the above results will be conserved, and that our total energy would be accurate to within a few per cent.

(ii) The ground state wavefunction, being the exponential of a quadratic function of the normal mode coordinates  $\xi_k$ , contains the correlations between the particles (inter- as well as intralayer), therefore this description would be better than any mean-field type of theory which cannot include correlation effects in a satisfactory way.

(iii) The neglect of the exchange in this calculation is justified for MLV less than about

30% [12]. In the solid phase, it is known that the MLV usually does not exceed 30% which can be used as a Lindemann criterion for melting of quantum systems [13]. So one can safely say that as long as one is in the *solid* phase, the exchange is negligible.

Our results are however qualitative since the quantum well has been approximated by a quadratic function in order to ease the diagonalization of the Hamiltonian.

Within this theory, the monolayer–bilayer transition was found as a function of the well width or the density. Due to the simple form of the Coulomb interaction, scaling relations were derived and a simple fitting formula was proposed for the total energy (classical + zero point) in the regime where the bilayer is stable. It was also deduced that for large  $x$  interlayer correlations become very small; the potential seen by the other layer is almost flat. The presence of the ‘optical’ mode at the  $\Gamma$  point ( $k = 0$ ) can be considered as a signature of the solid phase of the bilayer, and its discontinuities at structural transition points ( $x = 0.25, 0.61, 0.75$ ), although quite small, could presumably be observed in optical experiments. The mean square lattice displacements also become very large at these points; this suggests a re-entrant behaviour of the solid phase near these points.

In this paper, we only considered the case where the two layers had the same density. Experimentally, by changing the gate voltages, one can choose any arbitrary density in each plane. Our description in this case ceases to be valid in the sense that for small enough layer separation where the correlation effects become important, and in the case where the two densities are incommensurate, one would expect generation of defects such as dislocations and/or discommensurations to compensate for the lattice mismatch even at very low densities. Therefore the system would presumably not have long-range order in this case. Static defects such as remote donors [14] or impurities, as well as the substrate lattice mismatch, are expected to produce the same kind of effect. Work in this direction is under way.

## Acknowledgments

We acknowledge Dr Marcel Sluiter and Professor K Parlinski for useful discussions.

## References

- [1] McCombe B and Nurmikko A (ed) 1994 *Proc. 10th Int. Conf. on Electronic Properties of Two-Dimensional Systems; Surf. Sci.* 305
- [2] Bonsall L and Maradudin A A 1977 *Phys. Rev. B* 15 1959
- [3] Chui S T, Hakim T M and Ma K B 1986 *Phys. Rev. B* 33 7110
- [4] Esfarjani K and Chui S T 1991 *J. Phys.: Condens. Matter* 3 5825
- [5] Fisher D S 1982 *Phys. Rev. B* 26 5009
- [6] Esfarjani K and Chui S T 1991 *Solid State Commun.* 79 387
- [7] Esfarjani K 1991 *PhD Thesis* University of Delaware
- [8] Côté R and MacDonald A H 1990 *Phys. Rev. Lett.* 65 2662
- [9] Tanatar B and Ceperley D 1989 *Phys. Rev. B* 39 5005
- [10] Imada M and Takahashi M 1984 *J. Phys. Soc. Japan* 53 3770
- [11] The subroutine uncmnd.f which uses a quasi-Newton method was used to do the minimizations; see Kahaner D, Moler C and Nash S 1989 *Numerical Methods and Software* (Englewood Cliffs, NJ: Prentice-Hall)
- [12] This can be justified by comparing the exchange energy to the direct energy of two Gaussian wavefunctions. The ratio of the two would be proportional to  $\exp(-1/2\gamma^2)$  where  $\gamma$  is the ratio of the width of the Gaussian to the distance between the two Gaussian wavefunctions. For MLV =  $\gamma = 30\%$ , the ratio of exchange over direct Coulomb interaction is less than 0.004.
- [13] Chui S T and Esfarjani K 1991 *Europhys. Lett.* 14 361 and references therein
- [14] Chui S T and Tanatar B 1995 *Phys. Rev. Lett.* 74 458